

High-Density 2×4 Channel Polymer Optical Waveguide With Graded-Index Circular Cores

Yusuke Takeyoshi, *Student Member, IEEE*, and Takaaki Ishigure, *Member, IEEE*

Abstract—We propose to introduce a densely aligned 2×4 channel polymer parallel optical waveguide with graded-index circular cores for board-level optical interconnection, which is fabricated using the preform method. It is verified that this novel waveguide has sufficiently low loss (0.028 dB/cm at 850 nm and 0.061 dB/cm at 980 nm) and high bandwidth, due to the specific characteristic of the graded-index profile. This paper discusses insertion loss sensitivity to the displacement of the launched beam, various inter-channel crosstalk properties, and inter-channel skew, taking into account the real implementation of waveguides on printed circuit boards, especially for high-speed optical interconnects.

Index Terms—Graded-index profile, inter-channel crosstalk, optical interconnection, polymer waveguide, preform method, skew.

I. INTRODUCTION

DEMANDS for dense and high-speed interconnections between processing units or boards in high-end equipment such as core-routers, switches, and high-performance computers (HPCs) have increased as a result of growing Internet traffic and the technical progress of VLSI chips. Electrical interconnection technologies are not able to sufficiently meet these demands due to limitations in signal transmission rate, power dissipation, and wiring density. In order to overcome these bottlenecks, optical interconnections have been proposed and demonstrated [1]. This optical interconnect technology has already successfully been adopted for rack-to-rack applications, and actually demonstrates the extent of this technology's feasibility. Furthermore, in the last few years, the possibility of exploiting optics technologies has been considered even for inter-board and inter-chip applications [2]. In such ultra-short-reach interconnections, polymeric multimode optical waveguides have been widely used because of their ease of handling, flexibility, and cost-effectiveness. A wide variety of polymer materials have been explored for waveguides, and in general, most of the polymer waveguides have been prepared by photolithographic or imprinting techniques [3]–[5]. Due to the preparation process of those waveguides, almost all of the polymer waveguides have a square or rectangular core shape, and the refractive index of the core is uniform (step-index, SI). Since optical signals in those waveguides propagate by total internal reflection, the smoothness of the core-cladding

boundary has been a key parameter to reduce the scattering loss. In addition, having scattered light transfer to adjacent channels, i.e., inter-channel crosstalk, is of concern. In high-end equipment like HPCs, high-speed signal transmission with an extremely low bit error rate (BER) is required, to which end the propagation loss and inter-channel crosstalk should be reduced as much as possible.

In order to address these concerns in SI waveguides, we have reported the novel waveguide with four circular cores which have parabolic refractive index profiles (graded-index, GI) [6]. The parabolic refractive index profiles formed in the cores can effectively confine the optical signal around the core center, and thus the waveguides exhibit very low loss (0.028 dB/cm at 850 nm) and very high bandwidth (higher than 83 Gbps, which was experimentally measured using the time-domain measurement method with a 5-m-long waveguide), making them superior to conventional waveguides with square or rectangular cores with step-index (SI) profiles.

In addition to the low loss and low dispersion properties mentioned above, the possibility of higher density integration of GI waveguides, ultimately limited by alignment tolerances, is experimentally demonstrated, and compared to the waveguides with SI profiles. We also experimentally demonstrate that the GI cores can decrease the inter-channel crosstalk to less than -20 dB, even when the cores are aligned with extremely high density alignment, because of the tight confinement of the electrical field [7].

In this paper, we focus on the great advantages of the graded-index design in polymer parallel waveguides, followed by the fabrication process of a 2×4 channel waveguide. And then we describe the experimental results for loss, dispersion, inter-channel skew, and crosstalk under various conditions.

II. WAVEGUIDE FABRICATION

A large number of fabrication processes have been proposed for polymer waveguides [8]–[12], and most of them utilize lithographic processes or imprinting methods. Therefore, the shape of the cross-section of each core in polymer waveguides are generally designed to be square or rectangular, and the refractive index of the core region is uniform (i.e., step-index, SI, except for a few reports on GI type waveguides in the 1980s [13] whose main applications were coupler devices (not board-level optical interconnections)).

On the other hand, the waveguide we demonstrate in this paper is composed of cores with a circular shape, and each of them has a parabolic refractive index profile (i.e., graded-index, GI). In order to form such (multichannel) GI circular cores in a polymer waveguide, we utilize the preform process. We have

Manuscript received September 09, 2008; revised January 12, 2009. First published April 24, 2009; current version published July 15, 2009.

The authors are with the Faculty of Science and Technology, Keio University, Yokohama 223-8522, Japan (e-mail: takeyoshi@a5.keio.jp; ishigure@appi.keio.ac.jp).

Digital Object Identifier 10.1109/JLT.2009.2017385

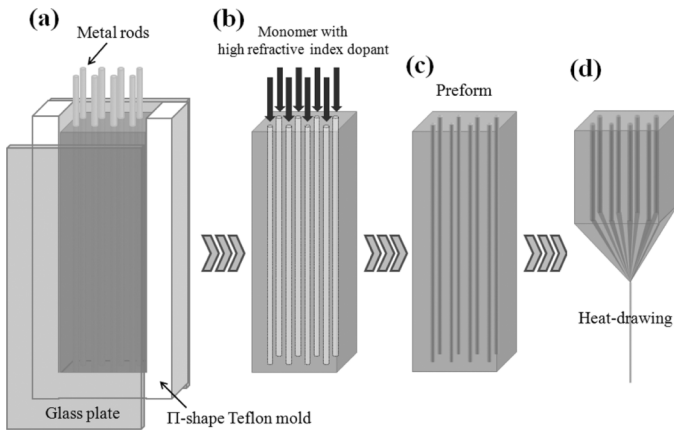


Fig. 1. Schematic representation of the fabrication process.

already reported the interfacial-gel polymerization technique as a fabrication process for preforms for high-bandwidth graded-index polymer optical fibers (GI POF) [14]. In the interfacial-gel polymerization process, a parabolic refractive index profile in the core region is automatically formed during the preform's polymerization procedure. In this paper, this preform preparation process was applied to make 2×4 channel parallel cores in the preforms for the novel waveguides.

The fabrication process of the 2×4 channel waveguide is schematically shown in Fig. 1. At first, an acrylic-polymer-based cladding with eight holes was prepared using stainless steel rods and a mold. The mold is composed of a Π -shaped frame made of Teflon and two glass plates. Fig. 1(a) illustrates the design of the mold used to prepare the claddings. Here, the number of stainless steel rods corresponds to the number of channels. Each stainless steel rod was wrapped by a fluoroplastic tube, and they were inserted into the guide holes made on the bottom of the Teflon mold. The diameter of the stainless steel rods and the position of guide holes were precisely determined from the waveguide structural design: core diameter, number of channels, and pitch. The stainless steel rods were then perfectly aligned to these guide holes.

Next, the mold was filled with the MMA monomer with a specified amount of polymerization initiator and chain transfer agent, and the subsequent polymerization reaction resulted in a plate-like polymer cladding. In order to prevent the cladding from containing bubbles, the polymerization reaction was carried out in an autoclave under high pressure (nitrogen gas atmosphere: 0.3 MPa.) After the polymerization reaction finished, the stainless steel rods and all the other parts of the mold were removed, to obtain the cladding ($50 \text{ mm} \times 13 \text{ mm} \times 300 \text{ mm}$, 2 mm ϕ holes), as shown in Fig. 1(b). The rods are easily removed from the polymer plate because of the small surface energy of the fluoroplastic that covers the rods. Next, the holes were filled with a mixture of acrylate monomer, high refractive index dopant (diphenyl sulfide: DPS), polymerization initiator, and chain transfer agent, in order to form parabolic refractive index profiles. Subsequently, the monomer in the holes was polymerized in an oil bath to obtain the preform [Fig. 1(c)]. Here, the concentration distribution of DPS (dopant) is automatically formed in each core, which corresponds to the index profile.

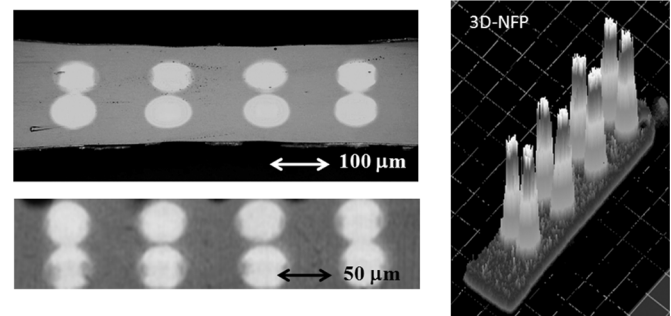


Fig. 2. Cross-sections of the fabricated 2×4 channel waveguide and NFP at the output end when all its channels are launched.

This method has been named as the interfacial-gel polymerization technique. The mechanism of forming the dopant concentration distribution is described in [14] in detail. The index profiles can be controlled by varying the polymerization temperature, polymerization time, or the amount of the dopants [15]. Finally, the preform was heat-drawn, like GI POF, to obtain the completed waveguide, as shown in Fig. 1(d). In this paper, we used a dopant concentration of 11% by weight in order to obtain a numerical aperture (NA) higher than 0.17. In our previous investigation of GI POF, we confirmed that an NA higher than 0.17 should be maintained in order to reduce mode coupling [16]. The reason we need to reduce mode coupling in the polymer waveguide newly developed is described in Section III.

After the preform was drawn to a waveguide, the cross-sectional shape (including the core shape and the size ratio of core and pitch) of the preform was perfectly maintained as shown in Fig. 2(a) and (b). We can obtain hundreds of meters of waveguide at one time from a 30-cm-long preform, and waveguides with a desired core diameter (over the range from 10 to $500 \mu\text{m}$) can be obtained by only varying the drawing speed. Fluctuation of the core diameter and the inter-core pitch is as low as several micrometers, if the molecular weight of PMMA is properly controlled. It can be seen in Fig. 2(a) and (b) that eight cores are well aligned, and the circular shape is maintained even after the heat-drawing; the core diameter of waveguide (a) is approximately $80 \mu\text{m}$, whereas waveguide (b) is $50 \mu\text{m}$. Fig. 2(c) shows the 3-D near field pattern (NFP) image of the eight-channel waveguide when all the channels are launched.

The horizontal and vertical inter-core pitches are approximately $190 \mu\text{m}$ and $80 \mu\text{m}$ in waveguide (a), and $120 \mu\text{m}$ and $50 \mu\text{m}$ in waveguide (b). Obviously, smaller pitch size is preferred for highly integrated parallel interconnections, and this preform process has a high degree of freedom in designing the pitch and core diameter in the waveguides. The vertically aligned cores of waveguides (a) and (b) could potentially be bundled into a single multicore optical core; this configuration allows for the most individual cores to be contained as densely as possible. One of the great advantages of leveraging a GI profile is that waveguide cores can be physically fused in a bundled configuration while staying optically isolated and not suffering from significant crosstalk.

Table I shows the specifications of waveguides (a) and (b).

TABLE I
SPECIFICATIONS OF WAVEGUIDE (a) AND (b)

	waveguide (a)	waveguide (b)
core diameter	80 μm	50 μm
horizontal inter-core pitch	190 μm	120 μm
vertical inter-core pitch	80 μm	50 μm
numerical aperture (NA)	0.17	0.17

III. RESULTS AND DISCUSSIONS

A. Refractive Index Profile

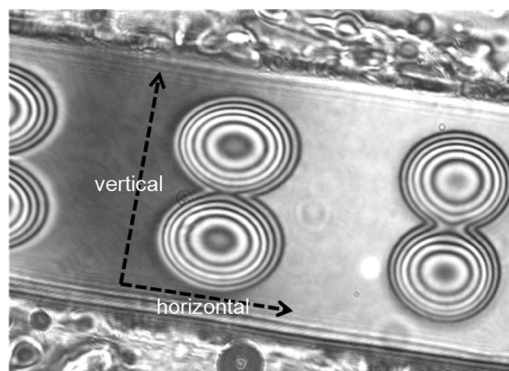
As mentioned above, a graded-index profile (parabolic profile) is automatically formed during core polymerization. The refractive index profile in each core was measured by an interferometric slab method. In this method, an incident light is divided into two light paths by a beam splitter and passes through a slab waveguide sample and a reference sample, and then, the interference of the two beams makes interference fringe patterns [17]. Fig. 3 shows an image of the cross-section of waveguide (b) (slab sample).

From Fig. 3(a), observed by the interference microscope (Mizojiri Optics, TD series), the circular core shape is also confirmed. Contour patterns of concentric interference fringes are observed in each circular core region, which indicate that a parabolic refractive index profile is obviously formed in each core region. The refractive index profiles of the four horizontally aligned cores and two vertically aligned cores, which are calculated from the fringe pattern, are shown in Fig. 3(b) and (c), respectively. It is also found from Fig. 3(c) that two vertically aligned cores overlap at their core peripheries. This core alignment design (without any inter-core spacing) could lead to ultimately high-density channel integration, if we could keep the inter-channel crosstalk low enough. Therefore, the crosstalk properties are investigated and explained in detail in Section III-F.

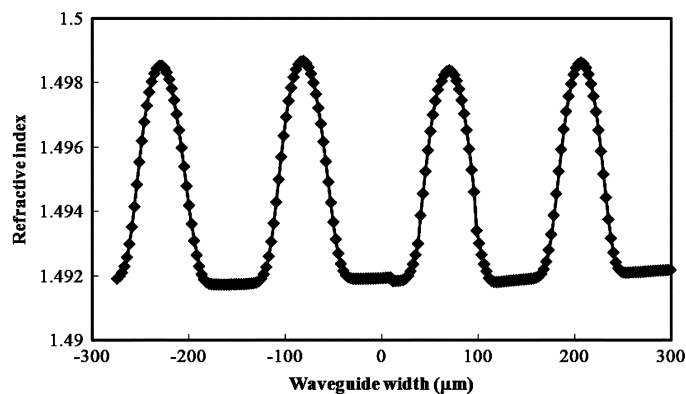
B. Propagation Loss at 850 and 980 nm

Very low BER signal transmission requires that the polymer waveguide has low loss, even though the transmission distance is short enough. However, the lasers most commonly used and commercially available for optical interconnection are vertical cavity surface emitting lasers (VCSELs) which mainly emit at a wavelength of 850 or 980 nm. In general, inexpensive and easily handled polymeric materials which include carbon-hydrogen bonds in them show relatively high absorption loss in infrared region, which increases the total propagation loss of polymer waveguides. Therefore, excess scattering loss caused by waveguide structures (e.g., the rough core-cladding boundary) should be reduced. In the case of GI core waveguides, unlike SI waveguides, the propagating modes in each core are so tightly confined around the core center that roughness at the core-cladding boundary should be negligible.

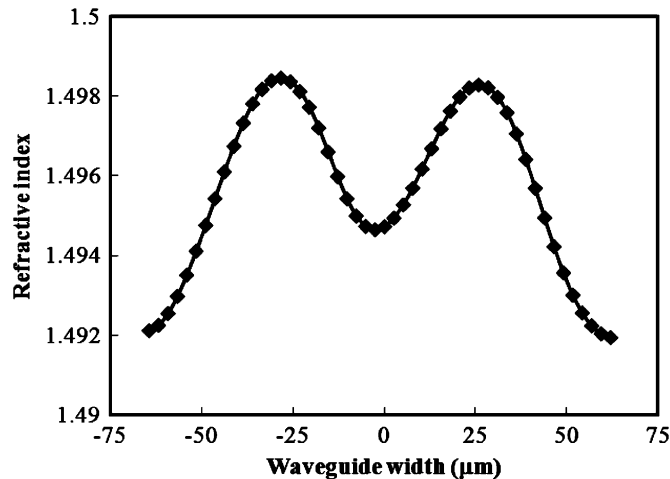
The propagation losses of waveguide (a) were measured by the cut-back method both at 850 nm and 980 nm. In this measurement, a 50- μm core multimode fiber (MMF) was utilized for launching a channel of the waveguide, and a 100- μm core MMF probe with an NA of 0.2 was used to guide the output light



(a)



(b)



(c)

Fig. 3. (a) Cross-sectional interference fringe pattern of an eight-channel waveguide. (b) Refractive index profile of four horizontally aligned channels. (c) Refractive index profile of two vertically aligned channels.

from the launched core to a detector. Fig. 4 shows the results of the cut-back process. (Note that the units of the horizontal axis are not “cm” but “m”.)

Losses at 850 nm and 980 nm were 0.028 dB/cm and 0.061 dB/cm, respectively. Although the waveguide is composed of general acrylic polymer (PMMA), its losses are sufficiently small, compared with the existing acrylic-polymer-based SI waveguides [3]. This is because the excess loss caused by the waveguide structure, such as an

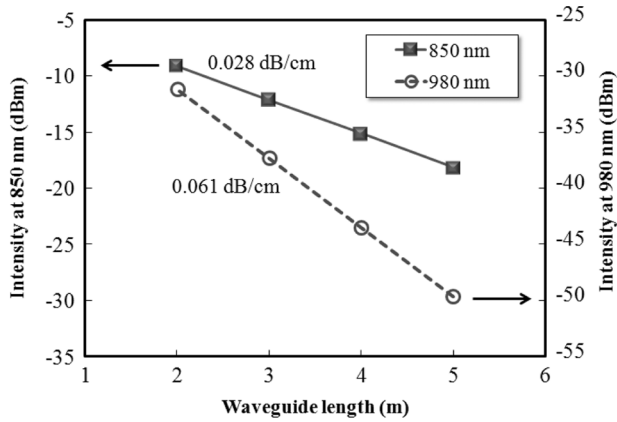


Fig. 4. Cutback plots of one channel at wavelengths of 850 and 980 nm.

irregular core-cladding boundary, is efficiently reduced in the GI cores, as demonstrated later in this paper.

In addition, the total coupling loss at the input and output ends was approximately 1.4 dB (0.7 dB at each end) at 850 nm without any index matching fluid, which was estimated from the intercept of vertical axis in Fig. 4. This estimated loss includes the loss due to the Fresnel reflection, scattering at rough surfaces of both ends, and mode mismatch. Since the core shapes of the new waveguide and probe fibers are similarly circular and have graded-index profiles, their modal power distributions could be much closer than those between rectangular SI core waveguide and probe fibers. Therefore, we posit that the circular core shape of this waveguide enables higher coupling efficiency, compared to the conventional SI waveguides. With respect to losses, the GI profile is significantly superior to the SI structure.

C. Gbps Signal Transmission

As one of the fundamental transmission properties, bandwidth as well as loss is a significant parameter for waveguides; hence, we investigated a high-speed signal transmission property of waveguide (a) using eye diagrams. The graded-index waveguide is expected to reduce modal dispersion, compared to the step-index waveguide, which would result in an error-free interconnection even at a transmission rate of 10 Gbps and beyond with low BER.

We demonstrated a 12.5-Gbps transmission through waveguide (a) as follows. A 12.5 Gbps $2^{31} - 1$ pseudorandom bit sequence (P.R.B.S.) signal was coupled to a commercially available VCSEL-based transmitter at 850 nm (California Scientific Inc., V-126) to modulate the light source. Then, the optical signal was sent through one channel of the waveguide via a 100- μm core MMF probe (1-m length), and the optical output from the channel was collected by a 100- μm core MMF probe to guide to a high-speed photo-receiver (California Scientific, Inc., P-101). These launching and detecting conditions are the worst condition for such a high-bit-rate transmission from the dispersion point of view, because almost all the modes in the core of the waveguide are launched. Under the overfilled mode launch condition, the optical signals would experience the largest intermodal dispersion. Fig. 5 shows the eye diagram measured after a 2-m-long transmission. Here, the persistent time was set to 1 s.

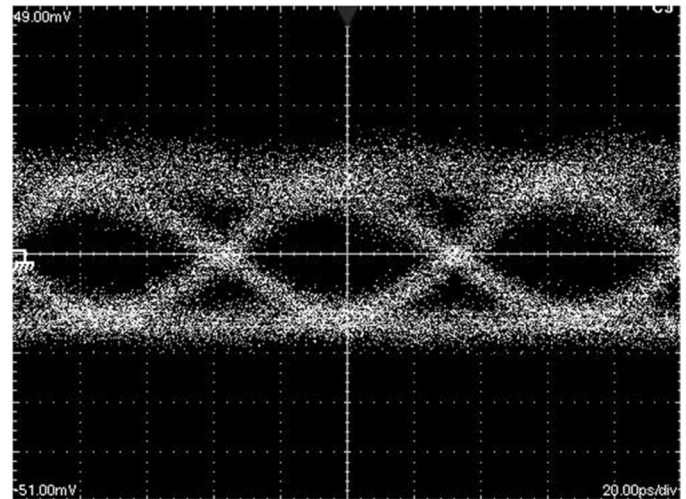


Fig. 5. Eye diagram at 12.5 Gbps after a 2-m-long waveguide transmission.

Despite the aforementioned severe launching and detecting conditions, no degradation of the eye opening is observed even after 2-m transmission (almost the longest transmission distance for the 10-Gbps error-free signal transmission due to the propagation loss). Thus, we confirm that the high transmission capability of the new waveguides results from its very low loss (~ 0.028 dB/cm) and reduction of modal dispersion achieved by the GI profile.

D. Tolerance for Displacement in Optical Coupling

From the viewpoint of the actual waveguide implementation, one of the key issues is a large tolerance in misalignment between the waveguide cores and the lasers [18]. However, in general, it is difficult to implement them without misalignment with low cost. Specifically, the GI profile may be disadvantageous in terms of this tolerance, because numerical aperture (NA) decreases in the radial direction from the core center. This local NA could result in the radial variation of coupling efficiency. In order to evaluate the effect of this coupling efficiency, we investigated how much the loss increases under such an offset launching condition as follows: we measured the output power when the center of a core was launched via a single mode fiber (SMF) probe. Then, the output power variation was evaluated by displacing the probe position from the center to the periphery by 1- μm steps. The offset displacement was in the direction along the lateral axis. The offset loss on the lateral axis displacement was measured on both waveguide (a) and waveguide (b), which have 80- μm cores and 50- μm cores, respectively (see Fig. 6).

These results indicate that, in the case of 80- μm diameter core [waveguide (a)], the displacement from the core center should be less than 20 μm (50% of its core radius) when assuming a 1-dB loss is allowed. Here, higher offset loss would be permitted for shorter required interconnection length (waveguide length).

Likewise, in the case of 50- μm -diameter core, it should be within 12 μm (50% of its core radius as well). Thus, we can conclude that the tolerance in misalignment between the center of the input beam and cores of waveguide is almost half size of the core radius, which would be large enough for the current integration techniques in printed circuit boards.

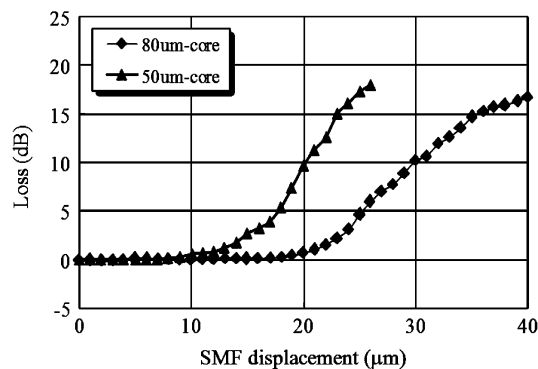


Fig. 6. Offset loss of waveguide (a) and (b).

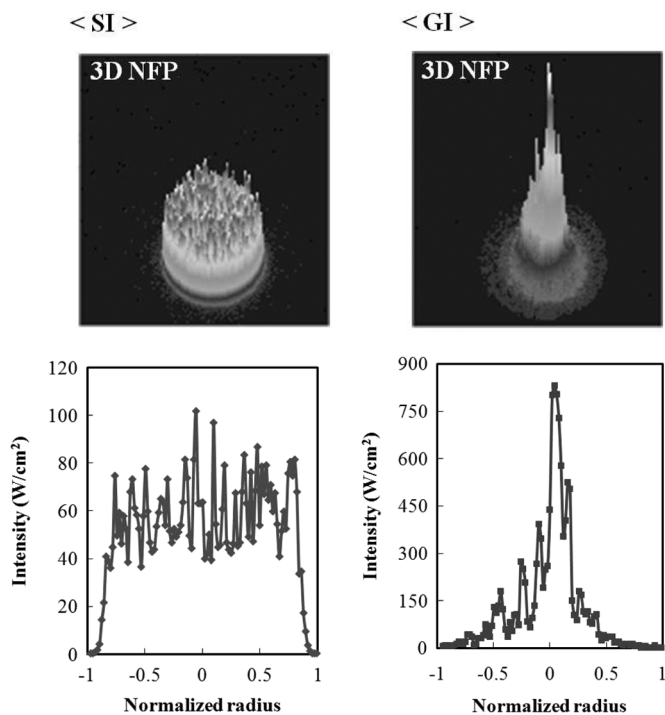


Fig. 7. Comparison of output optical field between SI and GI waveguide launched by MMF at 850 nm.

E. Optical Field Confinement by GI Profile

As we have discussed, the GI profile is expected to confine the electrical field of the propagating modes (i.e., optical field) around the core center, and this specific characteristic contributes to the low loss. We experimentally confirm the optical field confinement is achieved by a GI profile, compared to a step-index (SI) one. This comparison experiment was performed on the 250- μm core GI waveguide and the 240- μm core SI plastic optical fiber (SI-POF, MITSUBISHI, ESKA-240). The power distribution at the output ends of each waveguide (1-m length) was measured when launched by a 50- μm -diameter MMF probe (the center launch). Fig. 7 shows the near field patterns of each waveguide.

The output optical field of the SI-POF is almost uniformly extended to its entire core region in spite of the fact that only 4.3% of the core area is illuminated by the MMF probe. On

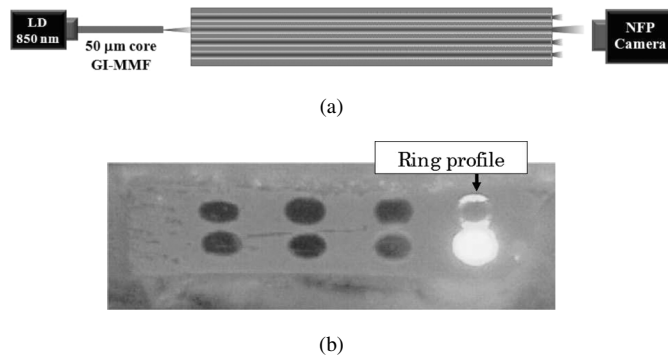


Fig. 8. (a) Schematic representation of measurement system. (b) Cross-sectional image of an eight-channel waveguide when the center of one edge core is launched.

the other hand, the output power distribution of the GI waveguide exhibits a parabolic shape similar to its index profile. Actually, it is calculated from the NFPs shown in Fig. 7 that 83% of the optical energy is concentrated within 125 μm of the core radius (50% of core radius) in the GI waveguide, while only 32% within 60 μm of the core radius in the SI POF (50% of core radius). This strong confinement achieved by the GI profile could enable highly integrated channel alignment, because even higher-order modes can be confined in the launched core and then inter-channel crosstalk can be reduced. This inter-channel crosstalk will be discussed in detail from the next section.

F. Inter-Channel Crosstalk

Signal light transfer to the other channels, mainly to the adjacent channels, is called crosstalk, and this unavoidable phenomenon can be a serious concern in a waveguide with densely aligned channels. In this section, various characteristic of crosstalk are discussed.

First of all, we investigated the inter-channel crosstalk after a 1-m-long waveguide transmission at 850 nm when only one channel was launched. The numerical aperture (NA) of each core is approximately 0.17 as summarized in Table I. Fig. 8(b) shows the cross-section after a 1 m transmission through waveguide (a) in which the center of an edge core was launched via a 50- μm diameter GI-MMF probe with an NA of 0.2 as shown in Fig. 8(a).

Optical power appears to be coupled to the unlaunched cores (i.e., crosstalk), particularly into the adjacent vertical ones, as shown in Fig. 8(b). However, it is noteworthy that the coupled power profile shows a ring pattern. This result indicates that the crosstalk signal is mainly coupled to the high-order skew modes of the unlaunched cores, because the ring pattern of NFP is the specific profile of high-order modes in conventional GI-POFs [16]. On the other hand, in the case of SI-POF, the NFP of all the modes are equally distributed over the core, which is independent of the launch condition. Therefore, if we adopt photo detectors with the effective area smaller than the core size of waveguides, this crosstalk with a ring profile in the GI waveguide would be spatially filtered. Consequently, with the optical field confinement effect shown in Fig. 7, very low crosstalk is expected in these new waveguides.

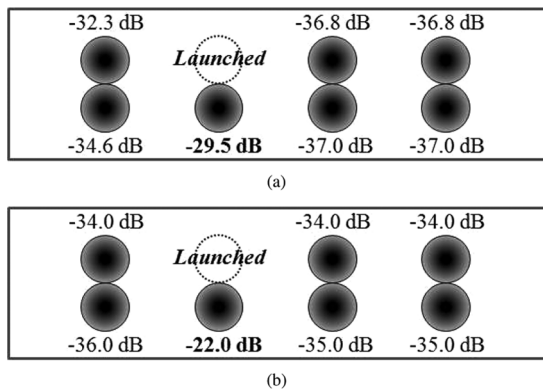


Fig. 9. Crosstalk values of each waveguide when only one core is launched by SMF at a wavelength of 850 nm. Waveguide (a): core 80 μm , vertical pitch 80 μm , horizontal pitch 190 μm , Waveguide (b): core 50 μm , vertical pitch 50 μm , horizontal pitch 120 μm .

Next, we quantitatively measured the crosstalk at 850 nm after propagation through two types of 1-m waveguides (a) and (b) when only one core in the eight-channel waveguides was launched. The crosstalk (dB) is defined as the ratio of output power from the launched core to that from an unlaunched core. In this measurement, a 9- μm -core SMF with a mode field diameter of approximately 9 μm , which was estimated from the cross-sectional NFP, was used as the launching probe [basically, the experimental setup is the same as Fig. 8(a)]. This SMF satisfies the single mode condition even at 850 nm. Here, the crosstalk was obtained by measuring the output signal power from the launched core and the coupled power to the other cores by utilizing a 1-m length 100- μm core GI-MMF with an NA of 0.2 as the detection probe for waveguide (a) and a 50- μm core GI-MMF with an NA of 0.2 for waveguide (b). Since the core diameter of the detection probes is almost the same as the core size of the measured waveguides and both detection probes have higher NA than the waveguides, the detection probe can collect almost all the optical power from the unlaunched core, which would be the worst detection condition from the crosstalk point of view. The results are summarized in Fig. 9.

Each value in Fig. 9 shows the crosstalk at the corresponding channel. From this figure, it is found that crosstalk power is as small as -20 dB and less in both waveguides despite the worst detection condition. The difference in crosstalk between waveguide (a) and (b) would depend on the different number of launched modes. What we particularly would like to emphasize here is that even the crosstalk to the vertically aligned core is still sufficiently small, although the vertical inter-core pitch is smaller than 100 μm in both waveguides (80 μm and 50 μm , respectively), and the outermost regions of the aligned core overlap together as shown in Fig. 3. Low-order modes launched by the SMF are confined only around the center of the launched core, and restrict the light leakage to the adjacent cores to about -22 dB. This outstanding crosstalk reduction is one of the largest advantages of waveguides with GI profiles, and it is expected to enable extremely high-density channel integration. Furthermore, the crosstalk is generally supposed to be higher with decreasing the inter-core distance, which was actually observed in conventional SI-core waveguides [19]. On the other

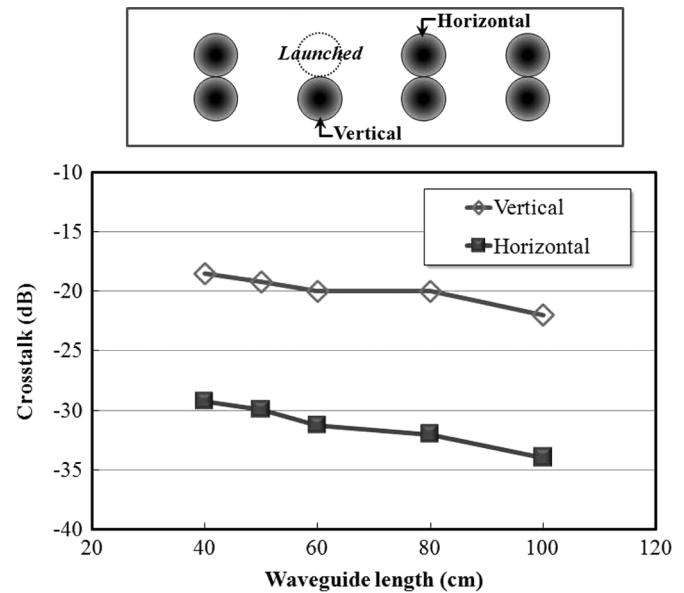


Fig. 10. Dependence of the crosstalk on propagation length.

hand, the crosstalk is independent of the inter-core distance in GI-core waveguides as indicated in Fig. 9. However, in the case of the GI core waveguides, the largest inter-core distance (ca. 400 μm) is not as large as that in the SI-core waveguide adopted in [12]. Therefore, further investigation is required on the dependence of crosstalk on inter-core distance.

Next, the dependence of the crosstalk on propagation length was measured, since crosstalk at various lengths of waveguide is an important characteristic for the actual integration of the waveguides on different kinds of printed circuit boards. In this measurement, waveguide (b) with 50- μm cores was investigated, and the signal wavelength was 850 nm. The same SMF as the one in the previous measurement was used for the launch probe, as well, and a 50- μm -diameter core GI-MMF was utilized as the detection probe, by which the core size of the probe could be the same as that of the measured waveguide. Fig. 10 shows the results of the dependence of crosstalk on propagation length with respect to a vertically contiguous core and a horizontal one as shown below.

The crosstalk gradually decreases with increasing the waveguide length in both cores. This result indicates that only a small amount of leaked power from the launched core couples to the adjacent (unlaunched) cores. As we already discussed, the leaked power is mainly coupled to the high-order skew modes, and those high-order modes have relatively high attenuation: they are often called leaky modes. Therefore, once the optical signal leaks out of the launched core, it barely couples to the other cores, but is weakly confined in the cladding of the waveguide. Actually, the slope of the plots in Fig. 10 signifies the attenuation of leaky modes. The slope of vertically aligned cores in Fig. 10 is smaller than that of horizontally aligned cores. This difference in slope is understandable because the leaked optical signal can easily couple to the vertically aligned contiguous core. However, in the range from 40 cm to 100 cm, crosstalk is small enough for a low BER transmission.

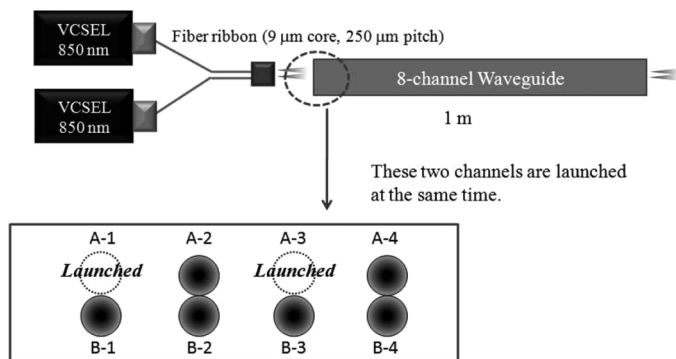


Fig. 11. Schematic representation of the experimental setup.

In this paper, we so far have described the crosstalk when only one channel is launched, but it is normally expected that all the cores need to transmit different optical signals by coupling the cores to VCSEL array transmitters. Therefore, we also evaluated the inter-channel crosstalk when several channels are launched simultaneously. Fig. 11 shows the experimental setup to measure the crosstalk under the simultaneous two-channel-launch condition.

In order to distinguish each core, the layers are labeled as A and B, and the columns are numbered from 1 to 4, as indicated in Fig. 11. As illustrated in Fig. 11, channels A-1 and A-3 of the 1-m-long waveguide (b) with $50\ \mu\text{m}$ cores were simultaneously launched by a four-channel fiber ribbon. The fiber ribbon was composed of single mode fibers with a core diameter and a pitch of $9\text{-}\mu\text{m}$ and $250\ \mu\text{m}$, respectively. Two different VCSEL light sources were connected to the two channels of the fiber ribbon, and their output ends were butt-coupled to waveguide (b). Since the pitch of waveguide (b) is $120\ \mu\text{m}$, the distance between the channels A-1 and A-3 is $240\ \mu\text{m}$, which is almost the same as the pitch of the fiber ribbon. Hence, the channels A-1 and A-3 could be launched, simultaneously. In principle, the way of measuring crosstalk is the same as that explained for Fig. 9.

Fig. 12 shows the experimentally measured 3-D NFPs under the conditions of single-channel-launch and the two-channel-launch.

From Fig. 12(a), it is obvious that the crosstalk to the unlaunched cores is almost negligible under the single-channel-launch, except for the contiguous channel B-1. On the other hand, under the two-channel-launch condition, crosstalk to all the unlaunched channels increases slightly. In addition, from Fig. 12(b), the increase of the crosstalk to the channels A-2 and A-4 is found to be approximately 3 dB; the crosstalk intensity doubles.

In contrast to this crosstalk increase in channels A-2 and A-4, the measured power at the originally launched channel (channel A-1) shows little change in “dB” unit system, because the increased power is no more than a thousandth part ($-30\ \text{dB}$) of the emitting power from the launched core. However, when all the channels (eight channels) are launched at the same time, the summed crosstalk ratio increases up to $-26\ \text{dB}$ in this waveguide, which implies that, in the case of the waveguide with so many channels, the accumulated crosstalk would reach a problematic level. Thus, the crosstalk is concerned in the parallel

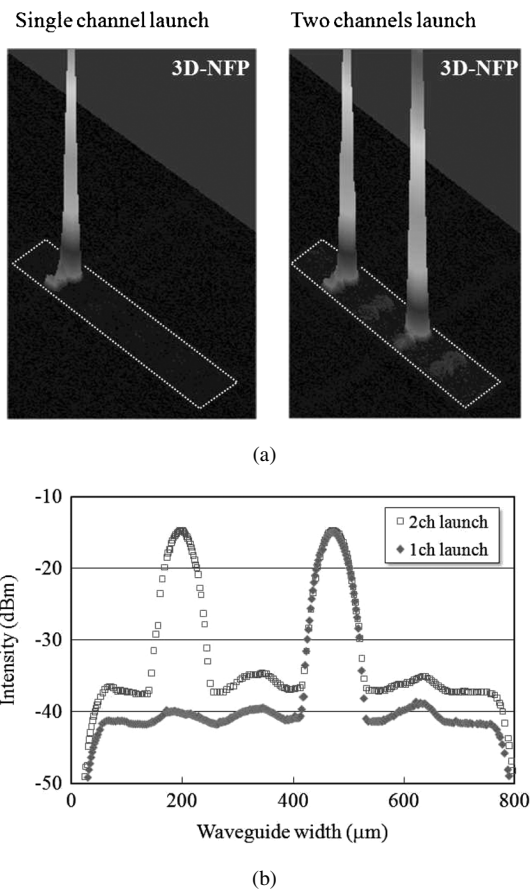


Fig. 12. (a) Comparison of 3-D NFP between one-channel-launch condition and two-channel-launch condition. (b) Comparison of intensity profile between one-channel-launch condition and two-channel-launch condition.

data transmission with a very low BER in high-end equipment. Therefore, the permissible crosstalk could be $-30\ \text{dB}$ and less. As a solution to the crosstalk problem, we proposed W-shaped index profile which has lower refractive index region around each core to reflect the leaked light from the adjacent channels [20]. We experimentally demonstrated that the waveguide with W-shaped index profile could reduce crosstalk to $-45\ \text{dB}$ or less. Therefore, if the system demands an extremely low BER signal transmission, applying the W-shaped index profile to each channel could be a promising solution.

We also investigate how crosstalk affects the eye diagram and BER. In order to provoke as high crosstalk as possible, waveguide (a) with $190\text{-}\mu\text{m}$ pitch was used for the measurement to intentionally inject light at the cladding region. This measurement setup is shown in Fig. 13.

In this measurement, the fiber ribbon was composed of multimode fibers with a core diameter and a pitch of $50\ \mu\text{m}$ and $250\ \mu\text{m}$, respectively. Three different VCSEL light sources (A), (B), and (C) were connected to the three channels of the fiber ribbon, and their output ends were butt-coupled to the waveguide (a). A 10.312-Gbps P.R.B.S. signal created by a pulse pattern generator (Anrits, MP1800A) was coupled to VCSEL (B) (JDS-Uniphase 10GBASE-SR XFP transceiver) while the others were modulated by 1-Gbps signals. As shown in Fig. 13, the 10.312-Gbps optical signals were coupled to

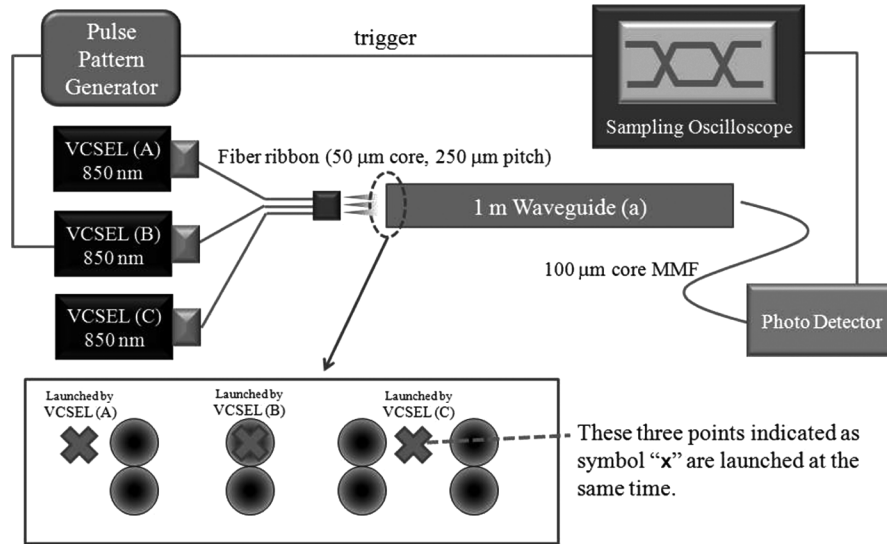


Fig. 13. Schematic representation of the experimental setup.

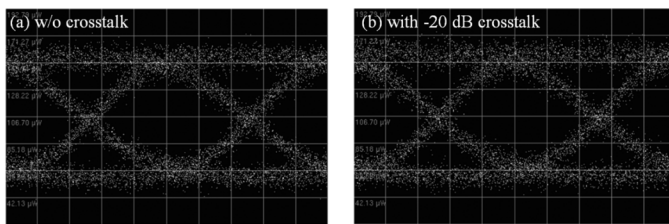


Fig. 14. Eye diagrams at 10 Gbps after a 1-m-long waveguide transmission. (a) No crosstalk. (b) With -20 -dB crosstalk.

the center of channel A-2, and the other two VCSELs (A) and (C), respectively, launched the cladding region to cause high crosstalk to channel A-2. The output light signal from channel A-2 was then collected by a $100\text{-}\mu\text{m}$ -diameter core MMF probe and guided to the photo detector (Anritsu, MU181640A) and the eye patterns were analyzed by a sampling oscilloscope (Anritsu, MP1026A). The persistent time was set to 1 second here. The total crosstalk to channel A-2 was -20 dB, since the output power from channel A-3 with and without crosstalk were -8.434 dBm and -8.480 dBm, respectively. The eye diagrams without and with -20 dB crosstalk are shown in Fig. 14(a) and (b), respectively.

As is obvious in Fig. 14, no difference can be observed between the two eye diagrams (a) and (b), which means crosstalk of -20 dB has little influence on the eye opening at a modulation speed of 10.312 Gbps. In addition, bit error ratio (BER) was also investigated and compared between two conditions. In terms of the BER as well as eye opening, no change was observed between the two conditions (error-free transmission was observed for more than 1-h operation). However, this crosstalk level could be a concern if a higher-bit-rate signal is transmitted through this waveguide and extremely low BER, i.e., less than 10^{-15} , is required. The effect of the crosstalk on BER characteristic should be accurately investigated, which will be published in elsewhere.

G. Inter-Channel Skew

In addition to the crosstalk properties discussed in Section III-F, inter-channel skew also needs to be reduced as much as possible to realize a high-bit rate parallel data transmission with low BER, because clock signals could be transmitted through one of the channels in a waveguide for parallel transmission systems. Compared to SI cores with uniform refractive index, our waveguide has a parabolic index profile in each core because of the concentration distribution of the dopants. Due to this formation process, the NA and index profile shape of each core could vary slightly from channel to channel, which can result in inter-channel skew. Thus, we quantitatively measured the inter-channel skew.

The inter-channel skew was measured with a picosecond pulsed laser (Hamamatsu, C8898) at 850 nm and a streak camera (Hamamatsu, C4334) as follows: first, a pulsed optical signal with 40 ps of FWHM was coupled to all the channels in the 1-m waveguide (a), simultaneously via a 1-m-long $1000\text{-}\mu\text{m}$ diameter SI POF probe with an NA of 0.3. Next, the output light from each core was introduced into the streak camera in order to measure the output pulse waveforms from all the channels simultaneously.

Fig. 15(a) and (b) shows the measured 2-D streak images. The lateral axis represents the distance along with the horizontal axis in the waveguide cross-section just drawn on the centers of the channels A-1 to A-4, as illustrated in Fig. 15(a). The vertical axis shows the time. Thus, the vertical width of the image indicates pulse broadening in time domain.

Fig. 16 shows the output pulses from each core on the upper layer A, obtained from Fig. 15. The inter-channel skew is defined as the difference in the arrival time of the peak position of output pulse. Table I summarizes the inter-channel skew for a 1-m transmission of layer A in waveguide (a).

As described in Table II, even the worst inter-channel skew was approximately 6 ps for the 1-m waveguide transmission

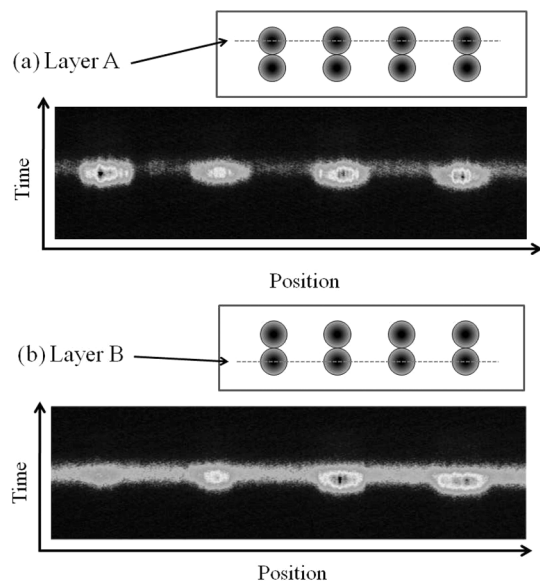


Fig. 15. 2-D images of output optical field.

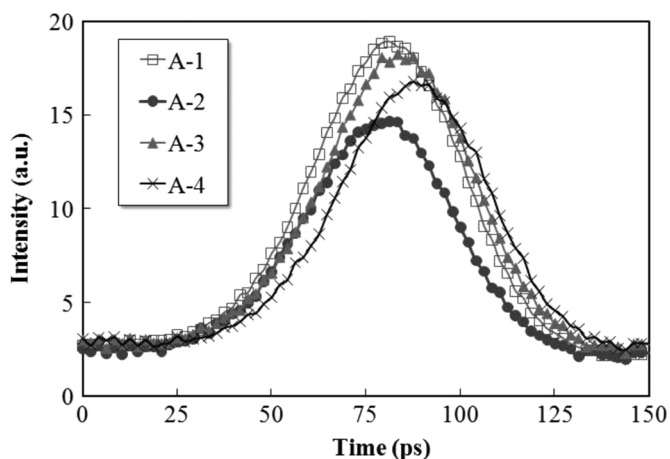


Fig. 16. Output pulses from each core on layer A after a 1-m transmission through waveguide (a).

TABLE II
SUMMARY OF INTER-CHANNEL SKEW

	A-1	A-2	A-3	A-4
A-1		0 ps	2.09 ps	6.26 ps
A-2			2.09 ps	6.26 ps
A-3				4.17 ps
A-4				

which is considered the longest transmission length for the actual board-to-board interconnection. Therefore, assuming 10-Gbps signals, since the time slot allotted for one bit is 100 ps in non-return to zero (NRZ) coding, the ratio of the skew to the time slot is only 6% even in the worst case (6 ps). Such a small skew is expected to be negligible. When it is presumed that skew could be permitted up to 25% of one bit time slot, our waveguide is capable of transmitting signals of 40 Gbps in parallel.

IV. CONCLUSION

A multimode 2×4 channel polymer optical waveguide with graded-index (GI) circular cores is presented. This waveguide exhibits low propagation loss (0.028 dB/cm at 850 nm, 0.061 dB/cm at 980 nm) and is capable of high-bit rate signal transmission, which is attributed to the GI-specific tight confinement of electrical field and reduction of modal dispersion. Furthermore, we demonstrate the outstanding crosstalk reduction in the ultimately dense channel alignment design (no spacing between neighboring channels), which is achieved by the tight confinement and prevention of inter-modal coupling from cladding modes to high-order modes. Toward the real implementation of waveguides in systems, crosstalk when multiple channels are launched simultaneously is investigated in detail. From this measurement, we find a possibility of data degradation by crosstalk even in the GI waveguides under the multichannel launch condition, because the summed crosstalk could reach -20 dB and beyond when all the channels are launched simultaneously. Thus, an application of W-shaped index profile to each core is highly desirable if a waveguide is designed to have many channels. Taking into account the operation in real systems, inter-channel skew is also investigated. Even if the worst skew is observed, approximately 40 Gbps parallel signal transmission can be achieved by our waveguide.

From these results, we conclude that application of graded-index profile to each core is a promising solution for high-density optical interconnection.

REFERENCES

- [1] A. F. Benner, M. Ignatowski, J. Lash, D. M. Kuchta, and M. Ritter, "Exploitation of optical interconnects in future server architectures," *IBM J. Res. Develop.*, vol. 49, no. 4/5, pp. 755–776, Sep. 2005.
- [2] D. M. Kuchta, Y. H. Kwark, C. Schuster, C. Baks, C. Haymes, J. Schaub, P. Pepeljugin, L. Shan, R. John, D. Kucharski, D. Rogers, M. Ritter, J. Jewell, L. A. Graham, K. Schrödinger, A. Schild, and H.-M. Rein, "120-Gb/s VCSEL-based parallel-optical interconnect and custom 120-Gb/s testing station," *J. Lightw. Technol.*, vol. 22, no. 9, pp. 2200–2212, Sep. 2004.
- [3] C. Berger, B. J. Offrein, and M. Schmatz, "Challenges for the introduction of board-level optical interconnect technology into product development roadmaps," *Proc. SPIE*, vol. 6124, 2006, 61240J.
- [4] Y. Tatara and H. Hosokawa, "Fabrication of replicated polymer optical waveguide," *Proc. OFC*, pp. 109–110, 2006.
- [5] D. Dobbelaere, P. Israel, P. V. Daele, P. Baets, R. Mohlmann, and G. R. Horsthuis, "Fabrication of vertical light couplers in polymeric waveguides by embossing," *Proc. LEOE*, pp. 178–179, 1994.
- [6] T. Ishigure and Y. Takeyoshi, "Polymer waveguide with 4-channel graded-index circular cores for parallel optical interconnects," *Opt. Express*, vol. 15, no. 9, pp. 5843–5850, Apr. 30, 2007.
- [7] Y. Takeyoshi and T. Ishigure, "Low inter-channel crosstalk property of 4-channel polymer parallel optical waveguide with circular GI cores," *IEEE Photon. Technol. Lett.*, vol. 19, no. 19, pp. 1430–1432, Oct. 2007.
- [8] R. Dangel, U. Bapst, C. Berger, R. Beyeler, L. Dellmann, F. Horst, B. Offrein, and G. L. Bona, "Development of a low-cost low-loss polymer waveguide technology for parallel optical interconnect applications," in *Proc. IEEE-LEOS Summer Top. Meet.*, San Diego, CA, 2004, pp. 29–30.
- [9] K. B. Yoon, C.-G. Choi, and S.-P. Han, "Fabrication of multimode polymeric waveguides by hot embossing lithography," *Jpn. J. Appl. Phys.*, vol. 43, no. 6A, pp. 3450–3451, Jun. 2004.
- [10] M.-H. Lee, X. Li, J. Y. Kim, J. Kang, S. Paek, and J. J. Kim, "Facile fabrication of polymer waveguide by using photosensitive polyimides," *Mol. Crystals Liquid Crystals*, vol. 377, pp. 7–12, 2002.
- [11] X. Wang, L. Wang, W. Jiang, and R. T. Chen, "Hard-molded 51 cm-long waveguide array with a 150 GHz bandwidth for board-level optical interconnects," *Opt. Lett.*, vol. 32, no. 6, pp. 677–679, Mar. 15, 2007.

- [12] C. Choi, L. Lin, Y. Liu, J. Choi, L. Wang, D. Haas, J. Magera, and R. T. Chen, "Flexible optical waveguide film fabrications and optoelectronic devices integration for fully embedded board-level optical interconnects," *J. Lightw. Technol.*, vol. 22, no. 9, pp. 2168–2176, Sep. 2004.
- [13] Y. Koike, Y. Takezawa, and Y. Ohtsuka, "New Interfacial-gel copolymerization technique for steric GRIN polymer optical waveguides and lens arrays," *Appl. Opt.*, vol. 27, no. 3, pp. 486–491, Feb. 1988.
- [14] T. Ishigure, E. Nihei, and Y. Koike, "Graded-index polymer optical fiber for high speed data communication," *Appl. Opt.*, vol. 33, no. 19, pp. 4261–4266, 1994.
- [15] T. Ishigure, S. Tanaka, E. Kobayashi, and Y. Koike, "Accurate refractive index profiling in a graded-index plastic optical fiber exceeding gigabit transmission rates," *J. Lightw. Technol.*, vol. 20, no. 8, pp. 1449–1456, Aug. 2002.
- [16] T. Ishigure, K. Ohdoko, Y. Ishiyama, and Y. Koike, "Mode coupling control and new index profile of GI POF for restricted launch condition in very short-reach networks," *J. Lightw. Technol.*, vol. 23, no. 12, pp. 4155–4168, Dec. 2005.
- [17] D. Marcuse, *Principles of Optical Fiber Measurements*. Norwell, MA: Academic, 1981.
- [18] N. Hendrickx, J. V. Erps, G. V. Steenberge, H. Thienpont, and P. V. Daele, "Tolerance analysis for multilayer optical interconnections integrated on a printed circuit board," *J. Lightw. Technol.*, vol. 25, no. 9, pp. 2395–2401, Sep. 2007.
- [19] I. Papakonstantinou, D. R. Selviah, K. Wang, R. A. Pitwon, K. Hopkins, and D. Milward, "Optical 8-channel, 10 Gb/s MT pluggable connector alignment technology for precision coupling of laser and photodiode arrays to polymer waveguide arrays for optical board-to-board interconnects," in *Proc. 2008 ECTC*, 2008, pp. 1769–1775.
- [20] Y. Takeyoshi and T. Ishigure, "Multichannel parallel polymer waveguide with circular W-shaped index profile cores," *IEEE Photon. Technol. Lett.*, vol. 19, no. 22, pp. 1795–1797, Nov. 2007.



Yusuke Takeyoshi (S'07) was born in Fukuoka, Japan, on August 8, 1984. He received the B.S. degree in applied physics and physico-informatics and the M.S. degree in integrated design functions from Keio University, Yokohama, Japan, in 2007 and 2009, respectively.

In April 2009, he joined Oracle Corp. Japan. His current research interests are in preparation and designing of polymer optical waveguide with graded refractive index profile towards high-speed and high-density optical interconnection.



Takaaki Ishigure (M'00) was born in Gifu, Japan, on July 30, 1968. He received the B.S. degree in applied chemistry and the M.S. and Ph.D. degrees in material science from Keio University, Yokohama, Japan, in 1991, 1993, and 1996, respectively.

He is currently an Associate Professor at Keio University. In 2005, he was with the Department of Electrical Engineering, Columbia University, New York, as a Visiting Research Scientist. His current research interests are in on-board optical interconnections realized with multimode polymer optical waveguides.